J. Chem. Eng. Data **2009,** *54,* 2701–2707

Equilibrium Adsorption Measurements of Pure Nitrogen, Carbon Dioxide, and Methane on a Carbon Molecular Sieve at Cryogenic Temperatures and High Pressures[†]

G. Watson,[‡] E. F. May,[*,‡] B. F. Graham,[‡] M. A. Trebble,[§] R. D. Trengove,[||] and K. I. Chan[⊥]

Centre for Petroleum, Fuels and Energy, School of Mechanical Engineering, University of Western Australia,
Crawley, WA, Australia 6009, Department of Chemical Engineering, Curtin University of Technology,
Bentley WA 6102, Australia, Separation Science Laboratory, Murdoch University, Murdoch WA 6150, Australia, and
Chevron Energy Technology Company, Houston, Texas 77002

A detailed experimental study of the adsorption behavior at equilibrium of pure nitrogen, methane, and carbon dioxide gases on a commercial carbon molecular sieve (Shirasagi MSC 3K-161) is reported at temperatures between 115 K to 323 K and pressures up to 5 MPa. A volumetric-type apparatus was used to obtain over 200 excess (Gibbs) adsorption capacity data over this range of pressure and temperature with an estimated uncertainty of 4 %. The absolute adsorption isotherms were type I in the IUPAC classification with the adsorption capacity at constant pressure increasing significantly with decreasing temperature. For each gas, the adsorption data were regressed to a four parameter Toth equation to represent the temperature and pressure dependence of the data with a relative standard uncertainty of 4 %. The optimized parameters from the Toth equation included the isosteric enthalpies of adsorption that were 17 $kJ \cdot mol^{-1}$, 27 $kJ \cdot mol^{-1}$, and 18 $kJ \cdot mol^{-1}$ for N_2, CO_2, and CH_4, respectively.

1. Introduction

Natural gas is the most environmentally friendly of the fossil fuels, and in contrast to many other clean fuels the infrastructure necessary for its widespread use already exists in many parts of the world. However, before a field can be developed the natural gas must be processed to remove impurities, and the cost of the required processing can be critical to the field's economic viability. Conventionally, CO_2 removal requires the use of a water-based amine solution and large absorber and regeneration towers. The capital and ongoing operational costs for this process are substantial, and the use (regeneration and disposal) of the amine solution can be problematic from the perspectives of both safety and the environment. Furthermore this conventional CO_2 removal process saturates the gas with water vapor and can require the duplication of expensive gas dehydration equipment; gas produced offshore is often dehydrated prior to being piped to an onshore processing facility to avoid hydrate formation. Once onshore, the acid gas removal processes must be followed by a repeat of the dehydration process using glycol contactors and, in cryogenic plants, molecular sieve towers.[1]

Nitrogen can also be a problematic impurity in natural gas. It is estimated that approximately 16 % of U.S. gas reserves are contaminated with higher amounts of N_2 than the 4 % by mole typically allowed by pipeline specifications.[2] In some liquified natural gas (LNG) plants, disposal of the end-flash vapor (excess to fuel gas requirements) can be hindered if it contains large concentrations of N_2 as the construction and operation of expensive cryogenic distillation towers to remove the nitrogen may be required. If a gas field contains CO_2 and N_2 at combined levels in excess of 10 % by mole, then the cost of conventional separation processes can make development of the field unviable.

Many workers are investigating the use of alternative gas separation technologies such as membranes and adsorption targeted at removing nitrogen or carbon dioxide from natural gas more efficiently.[2,3] Most of these investigations have focused predominantly on ambient temperatures or above.[4−15] Recently Bae and Lee[16] and Cavenati et al.[17,18] have reported equilibrium and kinetic sorption measurements with N_2, CH_4, and CO_2 on carbon molecular sieves to moderate pressures at ambient temperatures and above. However, very little work has been conducted studying the efficacy of adsorption processes at cryogenic temperatures and high pressures, and few adsorption equilibria data exist at these conditions even for simple conventional sieves; some examples are the works of Habgood[19,20] in 1958 and Lederman and Williams[21] in 1964. One aim of our research program is to help address this deficiency and produce adsorption equilibria data at low temperatures and pressures up to saturation. Such data would help in evaluating the feasibility of using pressure swing adsorption to separate nitrogen and carbon dioxide from methane at cryogenic temperatures.

This paper details the design and commissioning of the system that we have developed to characterize the equilibrium adsorption behavior at cryogenic temperatures of pure gases at pressures up to 7 MPa. We also present experimental adsorption isotherms for each of the pure gases N_2, CO_2, and CH_4 on a carbon molecular sieve (CMS), from 115 K to 323 K and at pressures up to 5 MPa, provided that the operating pressure is below the gas saturation temperature at the corresponding temperature.

---

[*] To whom correspondence should be addressed. E-mail: eric.may@uwa.edu.au.
[†] Part of the "William A. Wakeham Festschrift".
[‡] University of Western Australia.
[§] Curtin University of Technology.
[||] Murdoch University.
[⊥] Chevron Energy Technology Company.

10.1021/je900224w CCC: $40.75

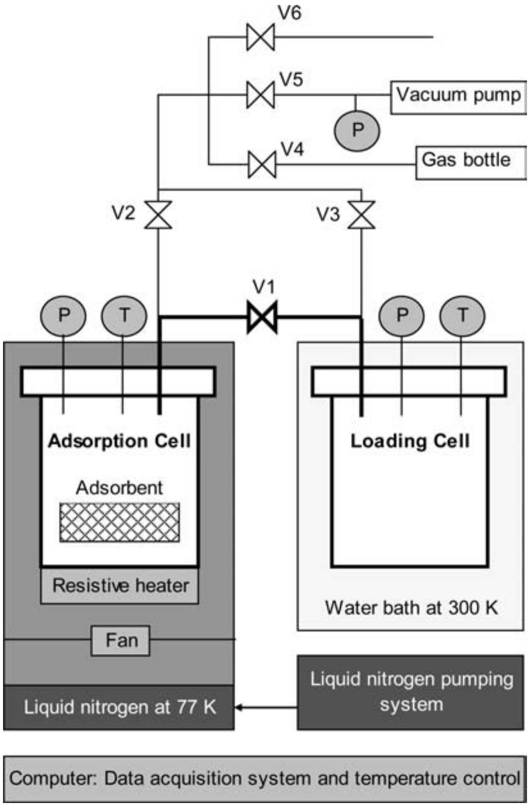

Figure 1. Schematic diagram of volumetric-type sorption apparatus.

2. Apparatus and Materials

A schematic of the volumetric-type apparatus used to measure the isothermal adsorption capacities is shown in Figure 1. It consisted primarily of two stainless steel pressure vessels, which we referred to as the adsorption cell and the loading cell. The adsorption cell had an internal volume of approximately 700 cm^3. The CMS was held in a basket made from stainless steel mesh suspended from the lid of the adsorption cell. The temperature of the adsorption cell was monitored with two 100 Ω platinum resistance thermometers (PRT), which were calibrated to ITS-90 over the range 77 K to 303 K with an estimated uncertainty of 0.08 K. (All uncertainties reported here are one standard uncertainty.) Both thermometers were mounted on the interior walls of the adsorption cell, one immediately adjacent to the basket holding the sieve, and the other on the cell's lid.

The adsorption cell was suspended from the lid of a cryogenic dewar and cooled by the boil-off vapor of a small amount of liquid nitrogen in the bottom of the dewar. The liquid nitrogen level was maintained at a constant value using an autonomous liquid nitrogen pumping system, and the boil-off vapor was prevented from stratifying by using a cryogenically compatible fan suspended from the bottom of the adsorption cell. An electrical resistance heater and a third PRT-100 element were mounted on the external surface of the cell and used in a Proportional Integral (PI) loop to control the cell's temperature. At steady state, the temperature stability of the adsorption cell was approximately ± 0.05 K; however steady-state thermal gradients were also observed with the two calibrated thermometers. These gradients dominate the temperature uncertainty of our data, which is estimated to be 1 K. Gas pressure in the adsorption cell was monitored by a quartz crystal transducer located outside the dewar with a full scale of 7 MPa and an estimated uncertainty over this range of 0.4 kPa.

The loading cell, which had an internal volume of approximately 1800 cm^3, was immersed in a stirred water bath maintained at ambient temperature. Its temperature was monitored using a PRT-100 element, calibrated to ITS-90 with an estimated uncertainty of 0.08 K, mounted on one of the internal walls. The uncertainty of the gas temperature inside the loading cell was estimated to be 0.1 K. Pressure in the loading cell was monitored by a second quartz crystal transducer with a full scale of 14 MPa and an estimated uncertainty of 0.8 kPa. The adsorption and loading cells were connected to each other, to their respective pressure transducers and to the gas handling manifold by 1/8 in. stainless steel tubing and high pressure valves and fittings. The total volume of these unthermostatted lines was estimated to be 5.7 cm^3, and thus their impact on the uncertainty of the adsorption measurements was less than 0.2 %. The temperatures and pressures measured by each of the aforementioned transducers were logged using commerical data acquisition software. The PI control loop for the adsorption cell temperature was also implemented in this software.

The following list of pure gases and supplier-reported purities (by mole) were used over the course of the measurements: He, 99.9995 %; Ar, 99.999 %; CH_4, 99.99 %; N_2, 99.999 %; and CO_2, 99.995 %. When changing the gas in the system, the cells and manifold were flushed several times by evacuating them to a pressure below 10 Pa (measured using a separate thermal convection vacuum gauge) and then pressurizing the system with the new gas to about 500 kPa (depending on the fluid's saturation pressure). The estimated uncertainty in the adsorption measurements due to gas purity was negligible.

The adsorbent used in this work was "Shirasagi MSC 3K-161" (Japan EnviroChemicals, Japan), a coconut-shell based carbon molecular sieve in the form of extruded pellets of cylindrical shape (length ≈ 4 mm, diameter ≈ 1.8 mm, lot number M683). This CMS has the same average micropore diameter as "Shirasagi MSC 3K-162",[18] which Bae and Lee[16] reported as being less than 4 Å with a BET surface area of 522.59 $m^2 \cdot g^{-1}$. Before introducing the adsorbent in the adsorption cell, the adsorbent was regenerated under vacuum (10 Pa) at 673 K for 24 h. The measured mass of regenerated CMS loaded into the cell was $m_{ads} = (41.17 \pm 0.01)$ g.

3. Methodology and Analysis

3.1. Calibration of the Loading Cell. The volumetric technique for measuring equilibrium adsorption capacities requires an accurate knowledge of the volumes of the vessels between which gas is being transferred. We therefore determined first the volume of the loading cell at ambient temperature. Then, prior to measuring the CMS isothermal adsorption capacity for N_2, CH_4, or CO_2, we determined the volume of the adsorption cell at the measurement temperature.

The volume of the loading cell was determined by connecting it to a separate gas cylinder containing approximately 1 MPa of either helium or argon. Before connecting it to the loading cell, the mass of the cylinder plus the gas it contained was measured using an electronic balance with a full scale of 1100 g and a resolution of 0.001 g. Gas was then transferred from the cylinder to the evacuated loading cell, and once equilibrium was reached, the loading cell was isolated and its pressure and temperature recorded. The gas cylinder was reweighed and the mass of gas transferred to the loading cell was calculated; a small correction was made to account for gas lost between the valves isolating the cylinder and loading cell. Approximately 2 g of helium or 30 g of argon were transferred, depending on the initial pressure in the gas cylinder. The reference equations of state (EOS) for helium[22] and for argon,[23] as implemented in the software REFPROP 8.0,[24] were used to calculate the gas density in the loading cell from the measured temperature and pressure. The loading cell volume was calculated from the mass transferred and the EOS densities with an estimated relative uncertainty of 0.2 %, based on the quadrature combination of the mass, temperature, pressure, and EOS uncertainties. The volume determination was repeated six times, thrice with helium and thrice with argon. The average of the six loading cell volume determinations was (1822 ± 2) cm^3.

Volume and Sorption Measurements. The volumetric method of measuring equilibrium adsorption capacity is based upon the transfer of a known amount of gas from one vessel (the loading cell) to another vessel containing the adsorbent (the adsorption cell). The two vessels constitute a closed system, and thus the material balance for the gas in the two vessels leads to

$$V_L(\rho(p,T)_L^{\text{init}} - \rho(p,T)_L^{\text{fin}}) + V_A(\rho(p,T)_A^{\text{init}} - \rho(p,T)_A^{\text{fin}}) + (n_{\text{ads}}^{\text{init}} - n_{\text{ads}}^{\text{fin}}) = 0 \quad (1)$$

Here, the subscripts “L” and “A” refer to measurements of the loading and adsorption cells, respectively; the superscripts “init” and “fin” refer to measurements taken before and after the gas was transferred, respectively; V is the cell volume; p is the measured cell pressure; T is the measured cell temperature; ρ is the molar gas density determined using an EOS at the measured pressure and temperature; and n_{ads} is the number of moles of gas adsorbed on the CMS. Once the volume of the loading cell was determined, it was necessary to determine V_A via helium calibration before eq 1 could be used to analyze subsequent experiments with N_2, CH_4, and CO_2 to determine n_{ads}.

The volume of the adsorption cell at each temperature was determined by transferring helium from the loading cell into the adsorption cell with a estimated relative uncertainty of 0.3 %. Fundamental to the volumetric technique is the widely used assumption that for helium at low pressures, $n_{\text{ads}} \equiv 0$.[25−29] The validity of this assumption may be questionable, particularly at cryogenic conditions;[30] however there does not to seem be any better method for this purpose at present. More importantly, an adequate objective of these measurements is to determine n_{ads} for N_2, CH_4, and CO_2 relative to helium, which this methodology achieves. At each temperature, we made several such helium transfers into the adsorption cell with p_A^{fin} ranging from 50 kPa to 400 kPa and the calculated value of V_A on each occasion was consistent within the estimated uncertainty. The apparent volume of the adsorption cell decreased slightly with temperature with $(1/V)(\Delta V/\Delta T) \approx 4 \cdot 10^{-5}\ \text{K}^{-1}$ over the temperature range studied. Corrections due to the compressibility of the adsorbent and the pressure vessel were negligible for our working pressures.[26]

Between each measurement of an adsorption isotherm, the adsorption cell was evacuated to a pressure below 10 Pa and heated to 353 K for a period of 24 h. Then the adsorption cell was returned to the required temperature with several hours required for stabilization. The loading cell was filled to a predetermined pressure with the pure gas of interest and then both cells were isolated from the gas handling manifold. The sorption isotherm was measured in two phases; for adsorption measurements, gas was transferred from the loading cell to the adsorption cell. Once the upper pressure on the isotherm was reached in the adsorption cell, the desorption phase of the measurement began with gas being transferred from the adsorption cell to the loading cell. After each transfer, which was enumerated by the index i, eq 1 was used to calculate $\Delta n_i \equiv (n_{\text{ads}}^{\text{fin}} - n_{\text{ads}}^{\text{init}})_i$. For $i = 1$, $n_{\text{ads}}^{\text{init}}$ was assumed to be zero (based on the lengthy period of evacuation and heating of the adsorption cell prior to the start of each isotherm).

Table 1. Equilibrium Sorption Data for Nitrogen on Shirasagi MSC 3K-161

p / kPa	Q_{ex} / mmol·g^{-1}	Q_{abs} / mmol·g^{-1}	p / kPa	Q_{ex} / mmol·g^{-1}	Q_{abs} / mmol·g^{-1}
$T = 298$ K					
150.5	0.42	0.42	5039.6	2.19	2.38
322.2	0.71	0.71	4185.8	2.13	2.29
505.4	0.93	0.94	1885.8	1.70	1.75
666.2	1.08	1.09	1586.7	1.60	1.64
883.6	1.25	1.26	1315.2	1.49	1.52
1093.2	1.37	1.39	1089.8	1.38	1.40
1318.1	1.48	1.51	881.9	1.25	1.27
1601.2	1.59	1.64	670.1	1.10	1.11
1959.3	1.71	1.76	491.6	0.93	0.94
2316.9	1.81	1.88	328.0	0.73	0.74
3289.0	2.02	2.14	154.8	0.44	0.44
3967.8	2.10	2.25			
$T = 248$ K					
229.0	1.28	1.28	2982.3	2.86	3.04
684.8	2.01	2.04	2630.2	2.81	2.96
1096.7	2.30	2.35	2300.1	2.71	2.84
1533.0	2.50	2.57	2031.7	2.66	2.77
1886.9	2.61	2.71	1757.2	2.60	2.69
2313.1	2.71	2.84	1509.2	2.53	2.61
2609.1	2.76	2.91	1249.7	2.45	2.51
3035.2	2.88	3.06	990.2	2.31	2.36
3570.7	2.90	3.12	822.5	2.20	2.24
4246.7	2.93	3.20	608.3	2.01	2.03
4611.8	2.95	3.25	397.8	1.74	1.75
4213.3	2.94	3.21	303.1	1.56	1.57
3554.8	2.90	3.13	159.3	1.18	1.18
$T = 198$ K					
95.1	1.89	1.90	3975.7	3.46	3.87
220.3	2.42	2.44	1862.5	3.47	3.64
409.9	2.80	2.83	729.2	3.12	3.18
623.1	3.03	3.08	298.2	2.62	2.64
1024.6	3.27	3.36	135.1	2.12	2.13
2979.0	3.54	3.84	66.4	1.67	1.68
5023.7	3.36	3.89			
$T = 148$ K					
14.0	2.51	2.51	3785.1	4.17	5.00
122.7	3.68	3.70	2052.2	4.44	4.80
232.9	3.97	4.00	987.2	4.43	4.58
402.0	4.18	4.23	456.1	4.23	4.30
604.7	4.31	4.40	217.9	3.96	3.99
999.9	4.42	4.57	108.8	3.65	3.67
2912.9	4.35	4.93	57.7	3.33	3.34
4542.9	3.98	5.09			
$T = 115$ K					
0.01	2.54	2.54	798.2	5.41	5.62
8.9	4.26	4.26	1373.4	5.32	5.74
64.1	4.92	4.93	1115.8	5.27	5.58
152.6	5.17	5.20	631.4	5.40	5.56
246.6	5.32	5.38	336.7	5.40	5.48
347.8	5.40	5.48	179.6	5.31	5.35
440.8	5.42	5.53			

The amount of gas transferred between each step along the isotherm ranged between about 50 mmol at low pressures and 500 mmol at high pressures. The uncertainty of the reference EOS for N_2,[31] CH_4,[32] and CO_2[33] was negligible compared to the uncertainties of V_A and V_L and those of our pressure and temperature measurements. The cumulative excess surface adsorption Q_{ex}[25] on the CMS was then calculated using

$$Q_{\text{ex}} = \frac{\sum_i \Delta n_i}{m_{\text{ads}}} \quad (2)$$

Table 2. Equilibrium Sorption Data for Methane on Shirasagi MSC 3K-161

p / kPa	Q_{ex} / mmol·g^{-1}	Q_{abs} / mmol·g^{-1}	p / kPa	Q_{ex} / mmol·g^{-1}	Q_{abs} / mmol·g^{-1}
$T = 298$ K					
241.5	1.45	1.46	3716.2	3.01	3.24
550.3	1.96	1.98	3023.9	2.94	3.12
848.5	2.25	2.29	2484.0	2.87	3.01
1124.5	2.43	2.48	1981.9	2.76	2.87
1377.5	2.54	2.61	1480.6	2.62	2.70
1610.3	2.63	2.71	1053.9	2.44	2.49
1883.6	2.74	2.84	831.8	2.29	2.33
2267.9	2.82	2.95	609.5	2.10	2.13
2659.5	2.88	3.04	503.1	1.98	2.00
3063.9	2.93	3.12	399.0	1.83	1.84
3740.8	2.98	3.22	306.7	1.66	1.67
4267.8	3.02	3.30	206.0	1.41	1.42
5155.6	3.03	3.37	105.5	1.02	1.02
4377.1	3.00	3.28			
$T = 248$ K					
43.5	1.45	1.45	3462.8	3.56	3.89
144.8	2.20	2.20	2293.2	3.55	3.76
382.8	2.79	2.81	1079.0	3.33	3.42
843.9	3.20	3.26	599.6	3.07	3.11
1588.9	3.44	3.57	505.7	2.98	3.02
2063.6	3.51	3.69	302.2	2.69	2.71
3131.6	3.59	3.88	147.0	2.25	2.26
4054.3	3.55	3.96	71.9	1.80	1.80
5046.2	3.48	4.02	40.3	1.46	1.46
4433.3	3.51	3.97	25.2	1.20	1.20
$T = 198$ K					
25.5	2.48	2.48	4499.1	3.70	4.67
112.7	3.31	3.32	3753.3	3.89	4.58
227.2	3.62	3.64	1992.5	4.13	4.41
427.7	3.86	3.91	827.4	4.05	4.15
624.9	3.98	4.05	324.4	3.76	3.79
1033.4	4.11	4.24	139.6	3.41	3.43
3004.7	3.98	4.45	63.8	3.04	3.05
$T = 148$ K					
38.4	3.56	3.56	701.0	4.35	4.48
115.6	4.05	4.07	813.7	4.32	4.48
201.2	4.23	4.26	574.7	4.37	4.48
293.2	4.31	4.36	273.9	4.28	4.33
403.5	4.36	4.43	128.9	4.11	4.13
505.3	4.37	4.46	64.9	3.91	3.92
603.8	4.36	4.48			

Table 3. Equilibrium Sorption Data for Carbon Dioxide on Shirasagi MSC 3K-161

p / kPa	Q_{ex} / mmol·g^{-1}	Q_{abs} / mmol·g^{-1}	p / kPa	Q_{ex} / mmol·g^{-1}	Q_{abs} / mmol·g^{-1}
$T = 323$ K					
10.9	0.34	0.34	4117.2	3.99	4.35
24.2	0.62	0.62	2004.7	3.77	3.91
94.7	1.42	1.42	1388.6	3.61	3.70
183.6	1.94	1.95	627.9	3.09	3.12
256.5	2.24	2.25	292.7	2.46	2.47
465.2	2.76	2.78	125.7	1.77	1.77
648.1	3.04	3.07	66.2	1.30	1.30
1668.4	3.68	3.80	38.8	0.98	0.98
3526.4	3.99	4.28			
$T = 298$ K					
12.1	0.72	0.72	4032.5	4.29	4.74
26.2	1.12	1.12	2313.3	4.29	4.50
96.3	2.08	2.09	1765.4	4.21	4.37
186.9	2.65	2.65	829.8	3.85	3.92
270.1	2.96	2.98	327.3	3.20	3.22
480.4	3.41	3.44	142.5	2.49	2.49
671.5	3.64	3.69	93.7	2.13	2.13
1786.4	4.13	4.29	54.5	1.69	1.69
3469.2	4.33	4.69			
$T = 273$ K					
16.6	1.47	1.47	2169.9	4.83	5.09
32.2	1.96	1.96	1376.4	4.69	4.84
110.2	3.05	3.05	740.6	4.45	4.52
259.4	3.81	3.83	340.1	4.00	4.03
535.1	4.26	4.31	153.0	3.36	3.37
719.5	4.42	4.48	81.9	2.84	2.84
1181.7	4.62	4.74	53.2	2.40	2.40
$T = 248$ K					
8.0	1.90	1.90	859.0	5.04	5.15
21.2	2.59	2.59	322.5	4.66	4.70
86.5	3.85	3.85	142.1	4.19	4.20
195.2	4.42	4.44	74.8	3.74	3.74
467.1	4.86	4.92	57.4	3.51	3.51
685.3	5.01	5.09	33.2	3.07	3.08
1107.5	5.16	5.30	25.2	2.84	2.85
$T = 223$ K					
1.8	1.73	1.73	440.9	5.49	5.55
4.9	2.61	2.61	315.2	5.38	5.42
11.7	3.43	3.44	191.6	5.20	5.23
81.6	4.78	4.79	91.9	4.88	4.89
303.7	5.35	5.39	52.3	4.60	4.60
515.1	5.54	5.61			

After each pressure change, equilibrium was considered to be reached when Δn_i was stable within 0.2 %. At pressures above 1 MPa, this criterion was usually achieved within 1 h, whereas at pressures below 100 kPa approximately 10 h was required. The repeatability of our Q_{ex} data along each isotherm (including adsorption and desorption steps) was better than 1 %. On the basis of an error propagation analysis, we estimate the average relative uncertainty of the Q_{ex} data to be 4 %.

To ensure that the values of Q_{ex} determined at each pressure by the cumulative application of eq 1 were not adversely affected by error propagation, a check measurement was made at the conclusion of the adsorption isotherm. The adsorption cell was re-evacuated and then gas was transferred to it from the loading cell, causing a pressure increase of between 1 and 2 MPa. The value of Q_{ex} at the equilibrium pressure obtained from this single transfer was always found to be within 2 % of the value determined from the multiple small transfers.

To a first approximation, the term V_A in eq 1 was assumed to be constant for all pressures on the adsorption isotherm. However, this assumption ignores the volume occupied by the adsorbed phase, which increases with gas pressure, and causes the actual value of V_A available to the gas phase to decrease. The absolute adsorption capacity of the CMS, Q_{abs}, is obtained from Q_{ex} by correcting for the volume occupied by the adsorbed phase.[34]

$$Q_{abs} = \frac{Q_{ex}}{1 - \rho_{M,gas}/\rho_{M,ads}} \tag{3}$$

Here $\rho_{M,gas}$ and $\rho_{M,ads}$ are the mass densities of the gas phase and adsorbed phase, respectively. The density of the adsorbed phase cannot be measured directly but can be inferred using one of several different methods described in the literature.[28,34−36] We used the Ono−Kondo model[34] to obtain $\rho_{M,ads} = 0.354$, 0.701, and 0.996 g·cm^{-3} for CH_4, N_2, and CO_2, respectively. These densities were assumed to be independent of pressure and temperature. The values of $\rho_{M,ads}$ obtained with the various methods[34] (Ono−Kondo model, ZGR EOS, VDW covolume) vary by about 10 %, increasing the relative uncertainty of Q_{abs} to 5 %.

4. Results and Discussion

Measured values of the Q_{ex} and Q_{abs} for the CMS as a function of temperature and pressure are presented in Table

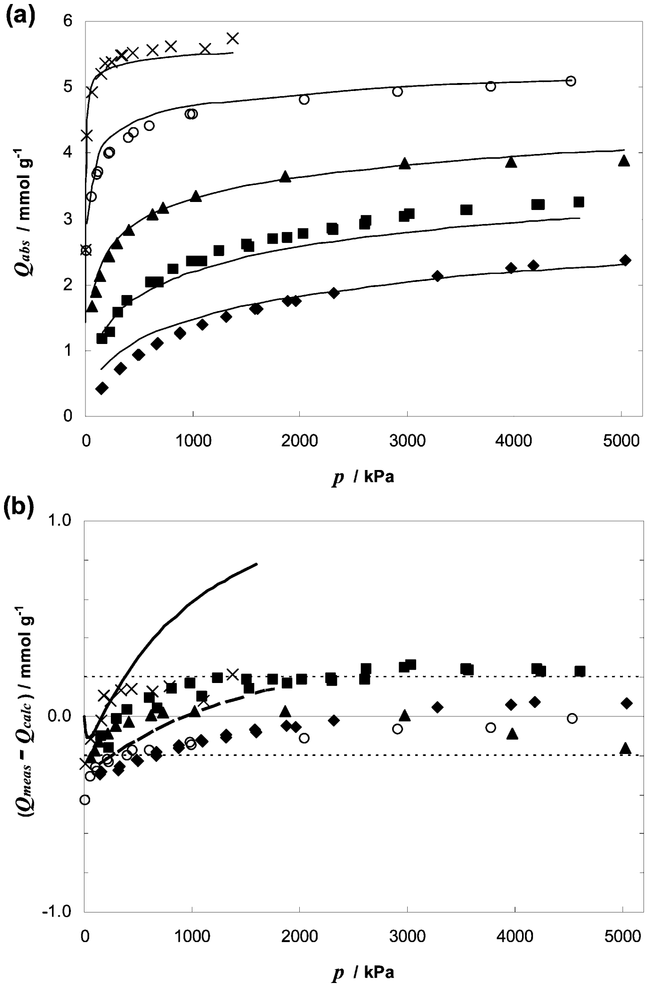

Figure 2. (a) Isothermal absolute adsorption data for N_2 on Shirasagi MSC 3K-161 measured in this work: ◆, 298 K; ■, 248 K; ▲, 198 K; ○, 148 K; ×, 115 K; and —, absolute adsorption capacity Q_{calc} determined using eq 4 with the N_2 parameters listed in Table 4. (b) Deviations ($Q_{meas} - Q_{calc}$) for the Q_{meas} data shown in (a) and from two literature sources. ---, estimated uncertainty, this work; —, ref 16 (293 K); — — —, ref 17 (298 K).

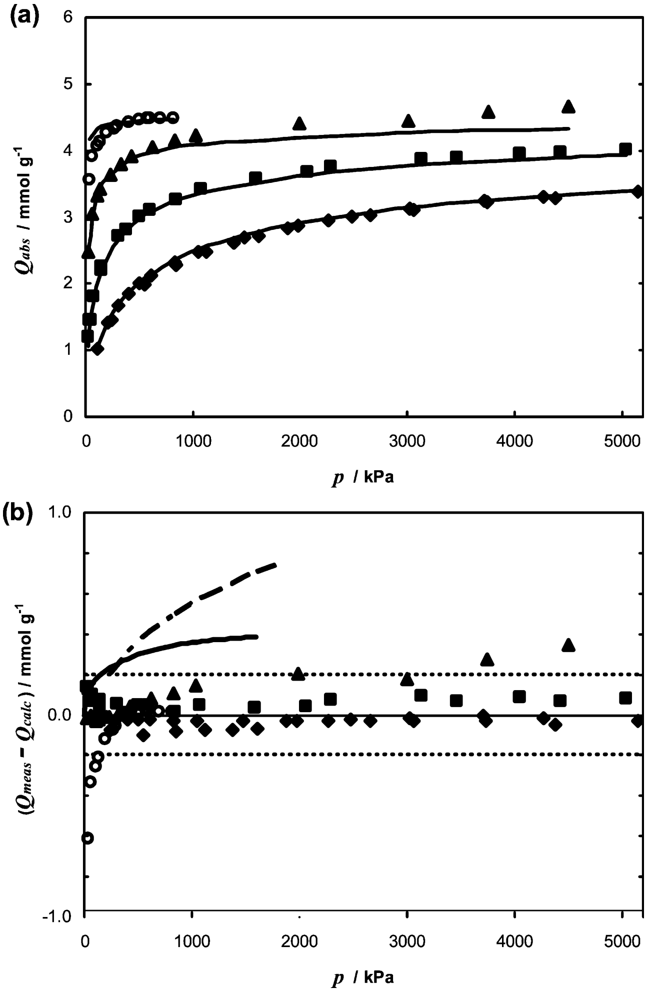

Figure 3. (a) Isothermal absolute adsorption data for CH_4 on Shirasagi MSC 3K-161 measured in this work: ◆, 298 K; ■, 248 K; ▲, 198 K; ○, 148 K; and —, absolute adsorption capacity Q_{calc} determined using eq 4 with the CH_4 parameters listed in Table 4. (b) Deviations ($Q_{meas} - Q_{calc}$) for the Q_{meas} data shown in (a) and from two literature sources. ---, estimated uncertainty, this work; —, ref 16 (293 K); — — —, ref 17 (298 K).

1 for N_2, in Table 2 for CH_4, and in Table 3 for CO_2. The measurement temperatures were 115 K, 148 K, 198 K, 248 K, and 298 K for N_2; 148 K, 198 K, 248 K, and 298 K for CH_4; and 223 K, 248 K, 273 K, 298 K, and 323 K for CO_2. The maximum pressure on each isotherm was either between 4000 kPa and 5200 kPa, or slightly below the gas saturation pressure at the corresponding temperature.

At low temperatures, some of the excess adsorption isotherms we measured exhibited a maximum; such maxima have been reported by many workers (for example Menon,[26] Zhou et al.,[36] and Sakurovs et al.[37]) and are a consequence of the increasing volume occupied by the adsorbed phase. As pressure increases, the excess adsorption typically increases to a maximum and then decreases linearly with increasing gas density, reaching zero again at the pressure where the gas density becomes the same as the adsorbed phase density.

In the top panels of Figures 2 to 4, the absolute adsorption isotherms are shown as a function of the pressure for each pure gas. Absolute adsorption increases with increasing pressure and decreasing temperature. The shape of these isotherms corresponds to type I in the IUPAC classification,[38] characterized by a saturation limit at high pressures when the micropores of the CMS are completely filled. For each gas, the repeatability of the adsorption data (measured as the pressure was increased) and the desorption data (measured as the pressure was decreased) was significantly better than the estimated uncertainty of the data. Thus the equilibrium sorption behavior of all three gases was completely reversible.

For each pure gas, the entire set of Q_{ads} data were regressed to the Toth equation[39]

$$Q_{abs} = Q_{max}\frac{Kp}{(1 + (Kp)^n)^{1/n}} \tag{4a}$$

$$K = K_0 \exp\left(\frac{-\Delta H}{RT}\right) \tag{4b}$$

Here R is the molar gas constant and ΔH is the isosteric enthalpy of adsorption. In the regression, ΔH was treated as an adjustable parameter along with the three empirical parameters Q_{max}, K_0, and n. The Toth equation is recommended for microporous adsorbents[40] because it has several advantages. It reduces to Henry's law in the limit of low pressure, it contains only four parameters, and it provides an analytical expression for the Q_{ads} that is an explicit function of temperature and pressure. The Toth equation

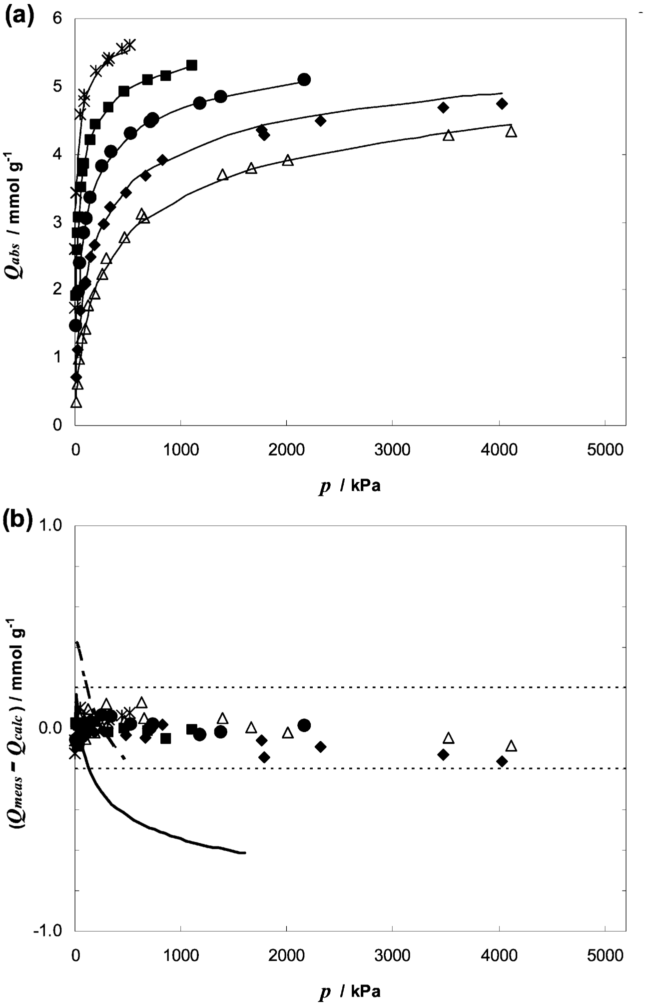

Figure 4. (a) Isothermal absolute adsorption data for CO_2 on Shirasagi MSC 3K-161 measured in this work: △, 323 K; ◆, 298 K; ●, 273 K; ■, 248 K; *, 223 K; and —, absolute adsorption capacity Q_{calc} determined using eq 4 with the CO_2 parameters listed in Table 4. (b) Deviations ($Q_{meas} - Q_{calc}$) for the Q_{meas} data shown in (a) and from two literature sources. ---, estimated uncertainty, this work; —, ref 16 (293 K); — — —, ref 18 (298 K).

Table 4. Toth Equation Parameters (Equation *4*) for the Absolute Adsorption Capacity of Shirasagi MSC 3K-161 for N_2, CH_4, and CO_2

gas		nitrogen	methane	carbon dioxide
no. of data		90	74	73
Q_{max}	mmol.g^{-1}	5.90 ± 0.13	4.551 ± 0.050	6.277 ± 0.071
$K_0 \cdot 10^6$	kPa^{-1}	12.9 ± 5.0	5.2 ± 1.3	0.590 ± 0.065
$-\Delta H$	kJ·mol^{-1}	17.23 ± 0.48	18.16 ± 0.50	26.81 ± 0.21
n		0.283 ± 0.017	0.501 ± 0.021	0.448 ± 0.010
stdev	mmol·g^{-1}	0.21	0.12	0.06
rel stdev		3.5 %	2.7 %	1.0 %

reduces to the Langmuir equation when the parameter $n = 1$; this parameter characterizes whether the gas adsorption on the adsorbent's surface is heterogeneous ($n \neq 1$) or homogeneous ($n = 1$).

The optimized parameter values resulting from the regression of eq 4 to each pure fluid data set are shown, together with their statistical uncertainties in Table 4. The relative standard errors of the fits ranged from 1 % for CO_2 to 3.5 % for N_2; all are smaller than the data's estimated relative standard uncertainty of 5 %. The deviation of our data from the regressed model are shown for all gases in the bottom panels of Figures 2 to 4. Systematic trends with decreasing temperature are apparent in the deviation plots, indicating that the model's functional form is not able to exactly describe the data within the precision of the data. Nevertheless, the model is more than adequate for the purpose of engineering design calculations.

Also shown in the bottom panels of Figures 2 to 4 are comparisons of our results with those of other workers who have investigated the adsorption of N_2, CH_4, and CO_2 on carbon molecular sieves from the same manufacturer. Bae and Lee[16] studied Shirasagi MSC 3A-162 using a volumetric-type apparatus at 293 K and pressures to 1.6 MPa. According to the manusfacturer, the equilibrium sorption properties of that CMS are very similar to those of the CMS studied in this work, although the two adsorbents differ in their kinetic properties.[41] Cavenati et al.[17,18] used a gravimetric-type apparatus to investigate the same adsorbent studied here for N_2 and CH_4 at 298 K at pressures to 2 MPa, and CO_2 at 298 K and 323 K at pressures to 0.5 MPa. (Cavenati et al. referred to their CMS as Takeda CMS3K, and Bae and Lee referred to their CMS as Takeda CMS-T3A. These names are now obsolete.[41]) The salient properties of the two adsorbents are given in refs 16 and 17, respectively; further information is also available from the manufacturer.[42]

In general, the data of Bae and Lee[16] and Cavenati et al.[17,18] deviate from the model fit to our data by between one and two times the estimated standard uncertainty of our results. However, Bae and Lee[16] and Cavenati et al.[17,18] only reported the model parameters which describe their data, rather than the data themselves or their uncertainties. It is difficult therefore to assess whether our data are consistent with theirs within the combined experimental uncertainties. Furthermore, in several cases the deviations between our data and those of Bae and Lee[16] or those of Cavenati et al.[17,18] are comparable in magnitude to the deviations between the two literature data sets. Since the deviations are in most instances not more than about twice our estimated uncertainty, it is plausible that the data of of Bae and Lee[16] and Cavenati et al.[17,18] might agree with ours within the combined uncertainty.

Fundamental adsorption data are critical to the evaluation of potential Pressure Swing Absorption separation processes based on particular adsorbents. This work represents the first stage in an ongoing effort to develop new experimental systems to measure the equilibrium and kinetic sorption phenomena of various adsorbents at cryogenic temperatures and high pressures. The capabilities of the apparatus described here are currently being extended to allow us to investigate such phenomena in multicomponent gas mixtures.

Acknowledgment

The authors thank Craig Grimm for helping to construct the apparatus and David Khouri for assistance with the measurements. The authors are also grateful to Reid Miller, David Trimm, Terry Edwards, Jeff Buckles, and Tony Eaton for their contributions to the project.

Literature Cited

(1) Kindlay, A. J.; Parrish, W. R. *Fundamentals of natural gas processing*; CRC Press: Boca Raton, 2006.
(2) Daiminger, U.; Lind, W. *Adsorption processes for natural gas treatment*; Engelhard Corp: Iselin, NJ, 2004.
(3) Hahn, P. R. Natural gas liquefaction with improved nitrogen removal. U.S. Patent 6,631,626 B1, 2003.
(4) Kuznicki, S. M. Preparation of small-pored crystalline titanium molecular sieve zeolites. U.S. Patent 4,938,939, 1990.
(5) Chao, C.-C.; Millwood, N. Y. Selective adsorption on magnesium-containing clinoptilolites. U.S. Patent 4,964,889, 1990.

(6) Ackley, M. W.; Yang, R. T. Adsorption characteristics of high-exchange clinoptilolites. *Ind. Eng. Chem. Res.* **1991**, *30*, 2523–2530.

(7) Fatehi, A. I.; Loughlin, K. F.; Hassan, M. M. Separation of methane-nitrogen mixtures by pressure swing adsorption using a carbon molecular sieve. *Gas. Sep. Purif.* **1995**, *9*, 199–204.

(8) O'Connor, D.; Barnes, P.; Bates, D. R.; Lander, D. F. A hydration-controlled nano-valve in a zeolite. *Chem. Commun.* **1998**, 2527–2528.

(9) Kuznicki, S. M.; Bell, V. A.; Petrovic, I.; Blosser P. W. Separation of nitrogen from mixtures thereof with methane utilizing barium exchanged ETS-4. U.S. Patent 5,989,316, 1999.

(10) Hernandez-Huesca, R.; Diaz, L.; Aguilar-Armenta, G. Adsorption equilibria and kinetics of CO_2, CH_4 and N_2 in natural zeolites. *Sep. Pur. Tech.* **1999**, *15*, 163–173.

(11) Kuznicki, S. M.; Bell, V. A.; Petrovic, I.; Desai, B. T. Small-pored crystalline titanium molecular sieve zeolites and their use in gas separation processes. U.S. Patent 6,068,682, 2000.

(12) Guest, J. E.; Williams, C. D. Efficient methane/nitrogen separation with low-sodium clinoptilolite. *Chem. Commun.* **2002**, 2870–2871.

(13) Jayaraman, A.; Hernandez-Maldonado, A. J.; Yang, R. T.; Chinn, D.; Munson, C. L.; Mohr, D. H. Clinoptilolites for nitrogen/methane separation. *Chem. Eng. Sci.* **2004**, *54*, 2407–2417.

(14) Delgado, J. A.; Uguina, M. A.; Gomez, J. M.; Ortega, L. Adsorption equilibrium of carbon dioxide, methane and nitrogen onto Na- and H-mordenite at high pressures. *Sep. Pur. Tech.* **2006**, *48*, 223–228.

(15) Maple, M. J.; Williams, C. D. Separating nitrogen/methane on zeolite-like molecular sieves. *Microporous Mesoporous Mater.* **2008**, *111*, 627–631.

(16) Bae, Y.-S.; Lee, C.-H. Adsorption kinetics of height gases on a carbon molecular sieve at elevated pressure. *Carbon* **2005**, *43*, 95–107.

(17) Cavenati, S.; Grande, C. A.; Rodrigues, A. E. Separation of methane and nitrogen by adsorption on carbon molecular sieve. *Sep. Sci. Technol.* **2005**, *40*, 2721–2743.

(18) Cavenati, S.; Grande, C. A.; Rodrigues, A. E. Upgrade of methane from landfill gas by pressure swing adsorption. *Energy Fuels* **2005**, *19*, 2545–2555.

(19) Habgood, H. W. The kinetics of molecular sieves action. Adsorption of nitrogen-methane mixtures by Linde Molecular Sieve 4A. *Can. J. Chem.* **1958**, *36*, 1384–1397.

(20) Habgood, H. W. Removal of nitrogen from natural gas. U.S. Patent 2,843,219, 1958.

(21) Lederman, P. B.; Williams, B. The adsorption of nitrogen-methane on molecular sieve. *AIChE J.* **1964**, *10*, 30–34.

(22) McCarty, R. D.; Arp, V. D. A new wide range equation of state for helium. *Adv. Cryo. Eng.* **1990**, *35*, 1465–1475.

(23) Tegeler, C.; Span, R.; Wagner, W. A new equation of state for argon covering the fluid region for temperatures from the melting line to 700 K at pressures up to 1000 MPa. *J. Phys. Chem. Ref. Data* **1999**, *28*, 779–850.

(24) Lemmon, E. W.; Huber, M. L.; McLinden, M. O. REFPROP - Reference Fluid Thermodynamic and Transport Properties, NIST Standard Reference Database 23, Version 8.0, **2007**.

(25) Sircar, S. Measurement of Gibbsian surface excess. *AIChE J.* **2001**, *47*, 1169–1176.

(26) Menon, P. G. Adsorption at high pressures. *Chem. Rev.* **1968**, *68*, 277–294.

(27) Keller, J. U.; Dreisbach, F.; Rave, H.; Staudt, R.; Tomalla, M. Measurement of gas mixture adsorption equilibria of natural gas compounds on microporous sorbents. *Adsorption* **1999**, *5*, 199–214.

(28) Dreisbach, F.; Losch, H. W.; Harting, P. Highest pressure adsorption equilibria data: measurement with magnetic suspension balance and analysis with a new adsorbent/adsorbate-volume. *Adsorption* **2002**, *8*, 95–109.

(29) Malbrunot, P.; Vidal, D.; Vermesse, J.; Chahine, R.; Bose, T. K. Adsorbent helium density measurement and its effect on adsorption isotherms at high pressure. *Langmuir* **1997**, *13*, 539–544.

(30) Gumma, S.; Talu, O. Gibbs dividing surface and helium adsorption. *Adsorption* **2003**, *9*, 17–28.

(31) Span, R.; Lemmon, E. W.; Jacobsen, R. T.; Wagner, W.; Yokozeki, A. A reference quality thermodynamic property formulation for nitrogen. *J. Phys. Chem. Ref. Data* **2000**, *29*, 1361–1433.

(32) Setzmann, U.; Wagner, W. A new equation of state and tables of thermodynamic properties for methane covering the range from the melting line to 625 K at pressures up to 1000 MPa. *J. Phys. Chem. Ref. Data* **1991**, *20*, 1061–1151.

(33) Span, R.; Wagner, W. A new equation of state for carbon dioxide covering the fluid region from the triple-point temperature to 1100 K at pressures up to 800 MPa. *J. Phys. Chem. Ref. Data* **1996**, *25*, 1509–1596.

(34) Sudibandriyo, M.; Pan, Z.; Fitzgerald, J. E.; Robinson, R. L., Jr.; Gasem, K. A. M. Adsorption of methane, nitrogen, carbon dioxide, and their binary mixtures on dry activated carbon at 318.2 K and pressures up to 13.6 MPa. *Langmuir* **2003**, *19*, 5323–5331.

(35) Murata, K.; Miyawaki, J.; Kaneko, K. A simple determination method of the absolute adsorbed amount for high pressure gas adsorption. *Carbon* **2002**, *40*, 425–428.

(36) Zhou, L.; Zhou, Y.; Bai, S.; Lü, C.; Yang, B. Determination of the adsorbed phase volume and its application in isotherm modeling for the adsorption of supercritical nitrogen on activated carbon. *J. Colloid Interface Sci.* **2001**, *239*, 33–38.

(37) Sakurovs, R.; Day, S.; Weir, S.; Duffy, G. Temperature dependence of adsorption of gases by coals and charcoals. *Int. J. Coal Geol.* **2008**, *73*, 250–258.

(38) Brunauer, S.; Deming, L. S.; Deming, W. E.; Teller, E. Theory of the Van der Waals adsorption of gases. *J. Am. Chem. Soc.* **1940**, *62*, 1723–1732.

(39) Toth, J. State of equations of the solid-gas interface layers. *Acta Chim. Acad. Sci. Hung.* **1971**, *69*, 311–328.

(40) Valenzuela, D. P.; Myers A. L. *Adsorption equilibrium data handbook*; Prentice-Hall: New York, 1989.

(41) Muto, N. Japan EnviroChemicals Ltd, Japan. Personal communication, June 2, 2008.

(42) Molecular Sieving Carbon/Carbon Molecular Sieve, Japan EnviroChemicals Ltd. http://www.jechem.co.jp/shirasagi_e/tech/msc.html (accessed April 17, 2009).

Received for review February 27, 2009. Accepted April 30, 2009. The research was funded by Chevron Energy Technology Company, the Western Australian Energy Research Alliance, and the Australian Research Council.

JE900224W